Mathematical and Experimental Analyses of Antibody Transport in Hollow-Fiber-Based Specific Antibody Filters

Mariah S. Hout[†,‡] and William J. Federspiel[*,†,‡,§,||]

The McGowan Institute for Regenerative Medicine and the Departments of Bioengineering, Chemical Engineering, and Surgery, University of Pittsburgh, Pittsburgh, Pennsylvania 15203

We are developing hollow fiber-based specific antibody filters (SAFs) that selectively remove antibodies of a given specificity directly from whole blood, without separation of the plasma and cellular blood components and with minimal removal of plasma proteins other than the targeted pathogenic antibodies. A principal goal of our research is to identify the primary mechanisms that control antibody transport within the SAF and to use this information to guide the choice of design and operational parameters that maximize the SAF-based antibody removal rate. In this study, we formulated a simple mathematical model of SAF-based antibody removal and performed in vitro antibody removal experiments to test key predictions of the model. Our model revealed three antibody transport regimes, defined by the magnitude of the Damköhler number *Da* (characteristic antibody-binding rate/characteristic antibody diffusion rate): reaction-limited ($Da \leq 0.1$), intermediate ($0.1 < Da < 10$), and diffusion-limited ($Da \geq 10$). For a given SAF geometry, blood flow rate, and antibody diffusivity, the highest antibody removal rate was predicted for diffusion-limited antibody transport. Additionally, for diffusion-limited antibody transport the predicted antibody removal rate was independent of the antibody-binding rate and hence was the same for any antibody−antigen system and for any patient within one antibody−antigen system. Using SAF prototypes containing immobilized bovine serum albumin (BSA), we measured anti-BSA removal rates consistent with transport in the intermediate regime ($Da \sim 3$). We concluded that initial SAF development work should focus on achieving diffusion-limited antibody transport by maximizing the SAF antibody-binding capacity (hence maximizing the characteristic antibody-binding rate). If diffusion-limited antibody transport is achieved, the antibody removal rate may be raised further by increasing the number and length of the SAF fibers and by increasing the blood flow rate through the SAF.

Introduction

Therapeutic antibody removal is performed to facilitate ABO blood group-incompatible kidney transplants (*1*) and heart (*2*) and kidney (*3*) xenotransplants (pig-to-baboon) and to treat Goodpasture syndrome (*4*), myasthenia gravis (*5*), hemophilia with inhibitors (*6*), and idiopathic thrombocytopenic purpura (*7*). Antibody removal is usually achieved nonselectively, via plasma exchange, or semiselectively, via plasma perfusion through immunoadsorption columns containing immobilized protein A or anti-human immunoglobulin (*8*−*12*). Most complications of plasma exchange are related to the replacement fluid; replacement with albumin solution may cause deficiency syndromes since beneficial antibodies and clotting factors are not replenished, while replacement with donor plasma may trigger hypersensitivity reactions or allow infectious disease transmission (*8*). Patients treated using protein A or anti-human immunoglobulin immunoadsorption columns benefit from semiselective IgG or IgM removal and require little to no replacement fluid (*9*−*12*). However, only a small fraction of the total antibody population (often only antibodies of one specificity) need be removed to effect the treatments listed above, and antibody removal platforms with even greater selectivity are desired.

We are developing hollow fiber-based specific antibody filters (SAFs) that selectively remove antibodies of a given specificity directly from whole blood, without separation of the plasma and cellular blood components and with minimal removal of plasma proteins other than the targeted pathogenic antibodies (*13, 14*). The working unit of the SAF is a hollow fiber dialysis membrane (dialysis fiber) with antigens, specific for the targeted antibodies, immobilized on the inner fiber wall. Several thousand SAF fibers are connected in parallel to produce a filter similar in construction to a hollow fiber hemodialyzer. During SAF-based antibody removal blood flows through the fiber lumens, and the targeted antibodies bind to the immobilized antigens and become trapped within the SAF. Nonspecific plasma protein adsorption is minimized by the use of hydrophilic cellulose-based SAF fibers.

Several studies have shown that SAFs and similar filters can selectively remove pathogenic antibodies and

* Ph: (412) 383-9499. FAX: (412) 383-9460. Email: federspielwj@msx.upmc.edu.
† The McGowan Institute for Regenerative Medicine.
‡ Department of Bioengineering.
§ Department of Chemical Engineering.
|| Department Surgery.

10.1021/bp025796f CCC: $25.00
Published on Web 07/23/2003

other substances from blood, plasma, and aqueous buffer. We have reported using SAF prototypes with immobilized A and B blood group antigens to remove anti-A and anti-B antibodies from whole human blood (*13*). Other groups have used similar dialysis fiber-based antibody filters with immobilized insulin (*15*), human IgG (*16*), and human albumin (HSA) (*16*) to remove anti-insulin antibodies from human plasma and anti-IgG and anti-HSA antibodies from rabbit serum and canine blood. Two groups have developed heparin filters composed of dialysis fibers with immobilized heparin-binding ligands: Yang et al. used filters with immobilized protamine to remove heparin from canine blood (*17*), and Ma et al. used filters with immobilized poly(L-lysine) to remove heparin from phosphate-buffered saline and bovine blood (*18*). Still other groups have developed antibody filters comprised of hollow fiber microfiltration membranes (microfiltration fibers) with antigens or protein A immobilized on the inner and outer fiber walls and on the surfaces of the pores within the fiber walls: Karoor et al. used filters with immobilized synthetic α-galactose (α-gal) antigens to remove anti-α-gal antibodies from human blood and plasma (*19*), and Klein et al. (*20*) and Charcosset et al. (*21*) used filters with immobilized protein A to remove human IgG from buffer. Microfiltration fiber-based antibody filters have higher antibody-binding surface areas (per unit of whole blood-contacting surface area) than do dialysis fiber-based antibody filters (like SAFs) but are more complex to operate than SAFs since partial separation of the plasma and cellular blood components occurs within microfiltration fiber-based filters. In each study described above, selectivity was demonstrated by showing minimal removal of the targeted antibodies or heparin by control filters (without immobilized antigens or heparin-binding ligands) (*13, 15, 17*−*19*) or by showing minimal removal of nontargeted antibodies or other plasma proteins by the test filters (with immobilized antigens or protein A) (*16, 20, 21*).

SAF-based antibody removal must be sufficiently fast as well as selective if the platform is to be clinically valuable. A principal goal of our research is to identify the primary mechanisms that control antibody transport within the SAF and to use this information to guide the choice of design and operational parameters that maximize the SAF-based antibody removal rate. In this study, we approached this goal by formulating a simple mathematical model of SAF-based antibody removal and performing in vitro antibody removal experiments to test key predictions of the model. The model describes radial diffusion and axial convection of antibodies in the fiber lumens, with reversible antibody−antigen binding at the fiber walls. In general, the model equations can be solved numerically to determine the antibody removal rate for a given SAF geometry, blood flow rate, antibody diffusivity, and antibody-binding rate. However, the model is substantially simpler if the characteristic antibody-binding rate is much larger or much smaller than the characteristic radial antibody diffusion rate. When antibody binding is much faster than antibody diffusion, antibodies that reach the fiber wall bind to antigens "instantaneously" and antibody transport to the fiber wall is limited solely by the radial antibody diffusion rate (i.e., antibody transport is diffusion-limited). Conversely, when antibody-binding is much slower than antibody diffusion, antibodies that bind to antigens are replaced "instantaneously" by diffusion of antibodies farther from the fiber wall, and antibody transport is limited solely by the antibody-binding rate (i.e., antibody transport is reaction-limited). For a given SAF geometry, blood flow rate, and antibody diffusivity, the antibody removal rate is highest when antibody transport is diffusion-limited. Additionally, when diffusion-limited antibody transport is achieved, the antibody removal rate is independent of the antibody-binding rate and hence is the same for any antibody−antigen system and for any patient within one antibody−antigen system.

The Damköhler number (*Da*) represents the ratio of the characteristic antibody-binding rate to the characteristic radial antibody diffusion rate (*22*): $Da = k_f c_s^i a/D$, where k_f (mL/nmol·s) is the intrinsic association rate constant for the antibody/antigen system, c_s^i (nmol/cm^2) is the initial surface concentration of antibody-binding sites on the SAF fiber (or the antibody-binding capacity of the fiber, the maximum surface concentration of bound antibodies attainable by the fiber), a (cm) is the inner radius of the SAF fiber, and D (cm^2/s) is the antibody diffusivity. We used the approximate surface concentration of a monolayer of IgG molecules, 0.004 nmol/cm^2 (0.6 μg/cm^2) (*23*), as an estimate for c_s^i. For a equal to 0.01 cm (*24*), D equal to 3.9×10^{-7} cm^2/s (*25*), and k_f between 0.01 and 100 mL/nmol·s (10^4 to 10^8 L/mol·s) (*26*−*28*), the Damköhler number for SAF-based antibody removal is between 1 and 10,000. Hence diffusion-limited antibody transport is achievable for medium to high affinity antibody−antigen systems ($k_f \geq 0.1$ mL/nmol·s or 10^5 L/mol·s), provided that the SAF fibers have enough antibody-binding sites to obtain near monolayer coverage of bound antibodies when the fibers are saturated.

Based on our expectation of diffusion-limited antibody transport, we chose to use a model antibody/antigen system for our in vitro antibody removal experiments instead of a human disease-related system. Use of the model system eliminated the need for a human source of antibodies and allowed all of the experiments to be performed using antibodies from one lot. We chose bovine albumin (BSA) as our model antigen, since BSA is a large molecular weight protein (*29*) like the ligands used in immunoadsorption columns (such as protein A and anti-human immunoglobulin) and can be immobilized on the SAF fibers using conventional protein immobilization methods. We used polyclonal anti-BSA antibodies as our model antibodies and compared both the magnitudes and the parameter dependencies of the measured anti-BSA removal rates to the predictions of our mathematical model. Finally, we used the information gained from our combined mathematical and experimental studies to suggest design, development, and operational approaches that can be taken to maximize the antibody removal rates achieved by SAFs developed for clinical use.

Antibody Transport Model

Model Geometry. The SAF is modeled as a bundle of N identical cylindrical fibers of length L (cm) and inner radius a (cm) (Figure 1). Antibody solution (blood, plasma, or buffer) enters the SAF at free antibody concentration c_i (nmol/mL) and flow rate Q (mL/min), and is distributed evenly among the fibers so that the flow rate through each fiber is Q/N. The shell compartment of the SAF (the space outside the fibers) is filled with isotonic buffer and closed. Within each fiber lumen antibodies undergo axial convection and radial diffusion, and at the fiber wall the antibodies bind reversibly to the immobilized antigens. Antibody solution exits each fiber at "mixing cup" free antibody concentration c_o (nmol/mL), and the antibody removal rate by the SAF R (nmol/min) is equal to the antibody solution flow rate Q multiplied by the difference between c_i and c_o.

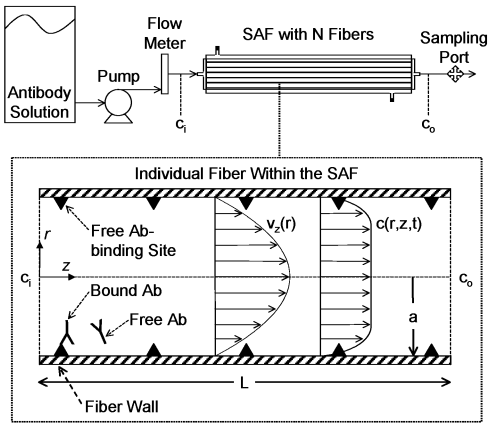

Figure 1. Perfusion system used during in vitro antibody removal experiments, with detail depicting antibody removal within the lumen of an individual SAF fiber. Ab: antibody.

Transport Formulation. The time-dependent mass conservation equation is used to describe the transport of free antibodies in each fiber lumen (*30*):

$$\frac{\partial c}{\partial t} + v_z\frac{\partial c}{\partial z} = \frac{D}{r}\frac{\partial}{\partial r}\left(r\frac{\partial c}{\partial r}\right) \tag{1}$$

where $c(r, z, t)$ (nmol/mL) is the concentration of free antibodies in the fiber lumen and $v_z(r)$ (cm/s) is the axial component of the antibody solution velocity (Figure 1). An initial condition and boundary conditions at the fiber wall, centerline, and inlet are required to solve eq 1 for $c(r, z, t)$. Additionally, an expression for the antibody solution velocity profile ($v_z(r)$) is needed.

Flow of blood, plasma, or buffer through a SAF fiber at a clinically relevant flow rate is laminar and fully developed, since the Reynolds number is small (<10 for buffer, plasma, or blood flow rates up to 500 mL/min through a dialyzer-sized SAF) and since the entrance length is less than 0.1% of the SAF fiber length (*31*). Hence the antibody solution velocity profile is parabolic (*30*):

$$v_z = 2v_{av}\left(1 - \frac{r^2}{a^2}\right) \tag{2}$$

where v_{av} (cm/s) is the average fluid velocity in the fiber (*30*). Though blood is a non-Newtonian fluid, the velocity profile for blood is parabolic at the shear rates likely to be encountered during flow through a dialyzer-sized SAF (*32*).

Initially, the SAF is primed with antibody-free isotonic buffer:

$$c = 0 \text{ at } t = 0 \tag{3}$$

At the inner fiber wall, the radial antibody flux is equal to the antibody-binding rate per unit of fiber surface area:

$$-D\frac{\partial c}{\partial r} = k_f c(c_s^i - c_b) - k_r c_b \text{ at } r = a \tag{4}$$

where k_r (s^{-1}) is the intrinsic dissociation rate constant for the antibody/antigen system. The antibody concentration profile in each fiber is symmetric with respect to radial position, and the antibody solution enters each fiber with a flat concentration profile:

$$\frac{\partial c}{\partial r} = 0 \text{ at } r = 0 \tag{5}$$

$$c = c_i \text{ at } z = 0,\ t > 0 \tag{6}$$

Finally, $c_b(z,t)$ is determined by integrating the radial antibody flux at the fiber wall over time:

$$c_b = \int_0^t -D\frac{\partial c}{\partial r}(r = a)\, dt \tag{7}$$

Dimensional Analysis. We used the dimensionless variables and parameters listed in Table 1 to simplify the solution and interpretation of the transport model. The dimensionless form of the mass conservation equation involves the Graetz number (Gz):

$$\frac{\partial c^*}{\partial t^*} + 2(1 - r^{*2})\frac{\partial c^*}{\partial z^*} = \frac{\pi}{Gz}\frac{1}{r^*}\frac{\partial}{\partial r^*}\left(r^*\frac{\partial c^*}{\partial r^*}\right) \tag{1a}$$

The Graetz number ($Gz = \pi a^2 v_{av}/LD$) represents the ratio of the characteristic radial diffusion time to the residence time (*30*). As Gz approaches infinity, $\partial c^*/\partial z^*$ approaches zero since the time required for the antibodies to diffuse to the immobilized antigens is much longer than the time the antibodies spend in the SAF. For a SAF with the same geometry as the prototypes used in our in vitro studies, the Graetz number for IgG removal ($D = 3.9 \times 10^{-7}$ cm^2/s (*25*)) is between 12.5 and 50.2 for antibody solution flow rates between 50 and 200 mL/min.

The dimensionless form of the wall boundary condition involves the Damköhler number (Da), described earlier:

$$-\frac{1}{Da}\frac{\partial c^*}{\partial r^*} = c^* - c_b^*\left(c^* + \frac{K_d}{c_i}\right) \text{ at } r^* = 1 \tag{4a}$$

where K_d (nmol/mL) is the equilibrium dissociation constant for the antibody/antigen system. As discussed earlier, the magnitude of the Damköhler number determines whether antibody transport is primarily controlled by the rate of antibody diffusion or by the rate of antibody-binding, or whether both rates are important. The dimensionless forms of the initial condition and the centerline and inlet boundary conditions are straightforward:

$$c^* = 0 \text{ at } t = 0 \tag{3a}$$

$$\frac{\partial c^*}{\partial r^*} = 0 \text{ at } r^* = 0 \tag{5a}$$

$$c^* = 1 \text{ at } z^* = 0,\ t^* > 0 \tag{6a}$$

The equation for the dimensionless bound antibody concentration involves the Graetz number and the ratio of the number of moles of free antibodies in one fiber volume ($V_f c_i$) to the number of moles of antibody-binding sites on the wall of one fiber ($A_f c_s^i$):

$$c_b^* = \frac{2\pi}{Gz}\frac{V_f c_i}{A_f c_s^i}\int_0^{t^*} -\frac{\partial c^*}{\partial r^*}(r^* = 1)\, dt^* \tag{7a}$$

where V_f (mL) and A_f (cm^2) are the volume and surface area of a single SAF fiber, respectively. Thus c_b^* rises slowly with time if the number of moles of antibody-binding sites on the fiber is large compared to the number of moles of antibodies in the antibody solution that fills the fiber. Also, c_b^* rises slowly with time if Gz is large,

Table 1. Dimensionless Variables and Groups

variable	description
$c^* = c/c_i$	free Ab concentration
$c_b^* = c_b/c_s^i$	bound Ab concentration
$r^* = r/a$	radial position
$z^* = z/L$	axial position
$t^* = t/(L/v_{av})$	time
$Gz = (\pi a^2 v_{av})/LD$	Graetz number
$Da = (k_f c_s^i a)/D$	Damköhler number

since $\partial c^*/\partial z^*$ is small for large Gz and most of the antibodies that enter the SAF leave without binding to antigen.

Simplification for c_b^* Near Zero. When c_b^* is near zero (i.e., far from saturation of the SAF), the unsteady term is removed from the mass conservation equation and the wall boundary condition is simplified:

$$2(1 - r^{*2})\frac{\partial c^*}{\partial z^*} = \frac{\pi}{Gz}\frac{1}{r^*}\frac{\partial}{\partial r^*}\left(r^*\frac{\partial c^*}{\partial r^*}\right) \qquad (1b)$$

$$-\frac{1}{Da}\frac{\partial c^*}{\partial r^*} = c^* \text{ at } r^* = 1,\ c_b^* = 0 \qquad (4b)$$

At the beginning of a SAF-based antibody removal session c_b^* is equal to zero. In general, c_b^* increases with time during the course of a session, but c_b^* may remain near zero throughout the session if the number of moles of antibody-binding sites within the SAF greatly exceeds the number of moles of antibodies initially present in the patient's blood.

Numerical Solution for c_b^* Near Zero. We used FlexPDE (PDE Solutions, Inc., Antioch, CA), a finite element-based partial differential equation solver, to obtain numerical solutions for $c^*(r^*, z^*)$ for any combination of Da and Gz and for c_b^* equal to zero. We then calculated the "mixing cup" antibody concentration at the SAF outlet, c_o (nmol/mL) (*30*):

$$c_o = c_i \int_0^1 c^*(1 - r^{*2})r^*\,dr^* / \int_0^1 (1 - r^{*2})r^*\,dr^* \qquad (8)$$

Finally we determined the antibody removal rate R (nmol/min) ($R = Q(c_i - c_o)$) and the antibody clearance K (mL/min) ($K = R/c_i = Q(1 - c_o/c_i)$). The clearance represents the volume of antibody solution completely depleted of antibodies per unit time, and is a more useful indicator of SAF performance than the antibody removal rate because the clearance depends only on the percent reduction in antibody concentration and is independent of the actual antibody concentration level in the blood (*33*). For c_b^* equal to zero, the governing equations are linear with respect to the free antibody concentration, and hence c_o is linearly proportional to c_i and the clearance is independent of c_i.

Analytical Solution for Large Da and c_b^* Near Zero. We obtained analytical solutions for $c^*(r^*, z^*)$, c_o/c_i, and K for large Damköhler number and for c_b^* equal to zero. As Da approaches infinity, the left side of eq 4b approaches zero and the wall boundary condition can be simplified:

$$c^* = 0 \text{ at } r^* = 1,\ c_b^* = 0,\ Da \to \infty \qquad (9)$$

Thus for large Da, antibodies that reach the fiber wall bind "instantaneously" and the free antibody concentration at the fiber wall is equal to zero. With this simplified boundary condition, we calculated $c^*(r^*, z^*)$ and c_o/c_i using the infinite series Graetz solution for radial diffusion in a circular tube with constant wall concentration (*34*). The solution in this limiting case ($Da \to \infty$) was designated the diffusion-limited solution, since the antibody removal rate was determined by the diffusion rate and was independent of the binding rate. The expressions for $c^*(r^*, z^*)$ and c_o/c_i and the needed eigenvalues, eigenfunctions, coefficients, and derivatives are presented in Skelland (*34*).

Materials and Methods

SAF Fabrication. Gambro (Lakewood, CO) 500 HG hemodialyzers were used as SAF modules. The modules contained approximately 6656 Hemophan hollow fiber membranes (regenerated cellulose with less than 1% of the surface hydroxyls replaced by diethylaminoethanol groups (*35*)) of 0.02 cm nominal inner diameter and 25.6 cm length (*36*). Bovine albumin (BSA) (Sigma Chemical Co., St. Louis, MO) or human albumin (HSA) (Alpine Biologics Inc., Orangeburg, NY) was immobilized on the lumenal surfaces of the fibers using a modified version of the cyanogen bromide activation method developed by Axen et al. (*37*). Unless otherwise noted, chemicals were obtained from Sigma Chemical Company (St. Louis, MO). During the following fiber activation steps, the blood and shell compartments of the SAF module were connected in series using Tygon tubing. Both compartments of the module were first rinsed copiously with deionized water. To swell the fibers, 3.5 L of 0.2 N NaOH was circulated through the module for 4 h, on ice, at 136 mL/min. The module was flushed with 3.5 L of 0.1 M sodium bicarbonate buffer/0.5 M NaCl, pH 8.3 (henceforth called bicarbonate buffer), at 225 mL/min and at 4 °C. An activating solution of 25 g of CNBr in 250 mL of 0.2 N NaOH was circulated through both compartments at 136 mL/min, on ice, for 1.5 h. The activating solution pH was kept above 11.0 by the addition of cold 10 N NaOH. The module was flushed with 3.5 L of deionized water and 3.5 L of bicarbonate buffer, at 225 mL/min and at 4 °C. Excess fluid was removed from the module using filtered compressed air.

The shell compartment was then filled with bicarbonate buffer and closed. One hundred milliliters of 20 mg/mL antigen solution (BSA, HSA, or a mixture of BSA and HSA, dissolved in bicarbonate buffer) was circulated through the blood compartment at 77 mL/min, at room temperature, overnight (at least 12 h). The concentration of BSA, HSA, or BSA/HSA in the antigen solution was determined by measuring the absorbance of the solution at 280 nm. Both compartments were drained, and the mechanical integrity of the fibers and the seal separating the blood and shell compartments was verified by checking for antigen in the buffer drained from the shell compartment. The blood and shell compartments were again connected in series, and the SAF was washed four times, by circulating 500 mL of bicarbonate buffer through the SAF at 136 mL/min for 1 h (each wash). Unreacted active sites on the fibers were capped by circulating 250 mL of 1 M ethanolamine, pH 8.3, through the SAF at 77 mL/min for 2 h. The SAF was flushed with 3.5 L of bicarbonate buffer (at 225 mL/min), 2 L of 0.1 M glycine pH 2.5 (at 77 mL/min), and 7 L of phosphate-buffered saline (PBS) (137 mM NaCl, 2.7 mM KCl, 10 mM Na_2HPO_4, 1.76 mM KH_2PO_4) pH 7.4 (at 225 mL/min). Finally, 3.5 L of PBS was circulated through the SAF at 136 mL/min overnight (at least 12 h). Excess fluid was removed from the SAF using filtered compressed air, and the SAF was stored at 4 °C until use.

Antibody Solution Preparation. Affinity purified, polyclonal sheep anti-BSA antibodies of IgG isotype were obtained from Bethyl Laboratories, Inc. (Montgomery, TX). The antibodies were supplied as a 1 mg/mL stock solution in PBS/0.1% NaN_3 and stored at 4 °C until use. For each antibody removal experiment, an appropriate volume of stock solution was added to PBS, pH 7.4, to obtain the desired concentration and volume of anti-BSA solution. All antibodies used were from the same lot.

Antibody Concentration Measurement. An in-house enzyme-linked immunosorbent assay (ELISA) (*38*) was used to measure the anti-BSA concentrations of samples collected during each experiment. Anti-BSA standards with concentrations between 2 and 40 ng/mL were prepared for construction of a reference curve. Each of the following solutions was added to the plate at 100 μL/well. BSA (10 μg/mL) in 0.1 M sodium carbonate buffer, pH 9.6, was added to each well of a high-binding Costar 96-well EIA plate (Fisher Scientific, Pittsburgh, PA), and the plate was incubated at 37 °C for 1 h. The plate was washed 5 times with 10 mM tris/100 mM NaCl/0.05% Tween 20, pH 7.4. The anti-BSA samples to be assayed (diluted appropriately in PBS/0.05% Tween 20, pH 7.4) and the anti-BSA standards were added to the plate in duplicate, and the plate was incubated for 1 h at 37 °C and washed five times. Horseradish peroxidase-conjugated anti-sheep IgG antibodies (Bethyl Laboratories, Inc., Montgomery, TX), diluted to 1 μg/mL in PBS/0.05% Tween 20, pH 7.4, were added to the plate, and the plate was incubated for 1 h at room temperature and washed six times. TMB peroxidase substrate (KPL, Gaithersburg, MD) was added to the plate, and the plate was incubated for 15 min at 37 °C. Finally, 1 M phosphoric acid was added to the plate, and the optical density of each well was measured at 450 nm using a microplate reader (Molecular Devices, Sunnyvale, CA). The concentration of each test sample was calculated by comparison to the reference curve.

In Vitro Perfusion System. In vitro antibody removal experiments were performed using the simple perfusion system depicted in Figure 1. The system consisted of a glass antibody solution reservoir, a Masterflex peristaltic pump (Cole-Parmer Instrument Company, Vernon Hills, IL), a glass bead flow meter (Cole-Parmer Instrument Company), a SAF, and a sampling port at the SAF outlet. The components were connected using Tygon tubing. The shell compartment of the SAF was filled with PBS and closed, and the antibody solution was pumped solely through the blood compartment. The entire perfusion system, except the reservoir, was deaired and primed with PBS prior to the antibody removal experiment. At the start of the experiment the reservoir was filled with anti-BSA solution, and the solution was pumped through the blood compartment of the SAF at the prescribed flow rate.

In Vitro Antibody Removal Experiments. During each antibody removal experiment, approximately one L of antibody solution was pumped through a freshly fabricated SAF in single pass mode at constant flow rate. (A control SAF with immobilized HSA was the only SAF used in multiple removal experiments.) Eight 1 mL outlet samples and two inlet samples were collected and assayed for anti-BSA concentration. The clearance was calculated using the mean concentrations of both inlet samples and the second through eighth outlet samples. Negligible rise of the outlet anti-BSA concentration with time verified that c_b^* remained near zero during each experiment.

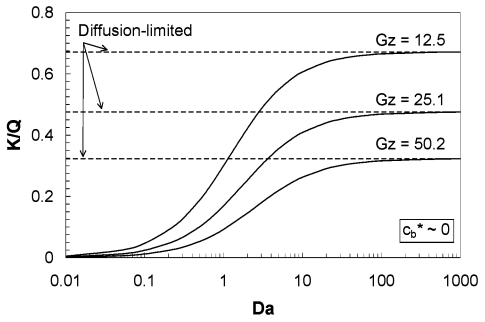

Figure 2. Predicted dependence of the dimensionless clearance (K/Q) on Damköhler number (Da), for Graetz numbers (Gz) equal to 12.5, 25.1, and 50.2. Dashed lines indicate the predicted dimensionless clearance for diffusion-limited antibody transport at each Graetz number. For each simulation the dimensionless concentration of bound antibodies is equal to zero.

The first series of experiments was performed to determine the dependence of antibody clearance on inlet anti-BSA concentration. Anti-BSA removal experiments were performed at inlet concentrations of 0.5, 1, and 2 μg/mL (0.0033, 0.0067, and 0.0133 nmol/mL), at a flow rate of 47 mL/min, using SAFs with immobilized BSA. The chosen anti-BSA inlet concentrations were within the range of specific antibody concentrations reported in the literature (*39*, *40*). To check for nonspecific anti-BSA removal, an experiment was performed using a SAF with immobilized HSA (which does not bind the anti-BSA used, data not shown), at an inlet concentration of 1 μg/mL and a flow rate of 47 mL/min.

The second series of experiments was performed to determine the dependence of antibody clearance on antibody solution flow rate. An anti-BSA removal experiment was performed at a flow rate of 110 mL/min and an inlet concentration of 2 μg/mL, using a SAF with immobilized BSA, and the measured clearance was compared to the previously measured clearance at 47 mL/min. Again the SAF with immobilized HSA was used to check for nonspecific anti-BSA removal at 110 mL/min. The flow rates used were of the same order as those used during hemodialysis (*36*).

The third series of experiments was performed to determine the dependence of antibody clearance on antibody-binding capacity. To fabricate a SAF with decreased anti-BSA-binding capacity, we used an antigen solution containing 10 mg/mL BSA and 10 mg/mL HSA. Using this SAF, we measured the clearance at an inlet concentration of 1 μg/mL and a flow rate of 47 mL/min, and compared the measured clearance to that measured for the SAFs with immobilized BSA only.

Results

Model Predictions. The numerically predicted dimensionless clearance K/Q ($K/Q = 1 - c_o/c_i$) increases nonlinearly with increasing Damköhler number and approaches the analytically predicted diffusion-limited dimensionless clearance as the Damköhler number approaches infinity (Figure 2). The dimensionless clearance represents the fraction of the flow through the SAF that is completely depleted of antibodies, and equals one if the antibody concentration at the SAF outlet equals zero. Figure 2 reveals the approximate boundaries of three antibody transport regimes, defined by the magnitude of the Damköhler number: reaction-limited ($Da \leq 0.1$), intermediate ($0.1 < Da < 10$), and diffusion-limited ($Da \geq 10$). The predicted dimensionless clearance is very low (<0.05) in the reaction-limited regime. In the intermedi-

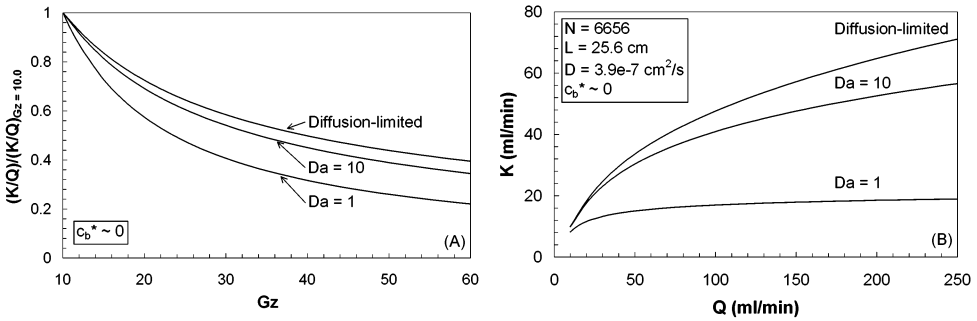

Figure 3. (A) Predicted dependence of the dimensionless clearance, relative to the dimensionless clearance at Graetz number (*Gz*) equal to 10.0 ($(K/Q)/(K/Q)_{Gz=10}$), on Graetz number, for Damköhler numbers (*Da*) of 1 and 10 and for diffusion-limited antibody transport. (B) Predicted dependence of clearance (*K*) on antibody solution flow rate (*Q*), for Damköhler numbers of 1 and 10 and for diffusion-limited antibody transport. The SAF geometry is identical to the geometry of the SAF prototypes used for in vitro experiments. For each simulation the dimensionless concentration of bound antibodies is equal to zero.

ate regime, the predicted dimensionless clearance is higher (up to 0.6 at *Gz* equal to 12.5 and *Da* equal to 10) and increases substantially with increasing Damköhler number. The predicted dimensionless clearance is highest in the diffusion-limited regime and increases very little with increasing Damköhler number. As expected from our earlier examination of eq 1a, for all Damköhler numbers the predicted dimensionless clearance is highest at the lowest Graetz number.

The rate at which the predicted dimensionless clearance decreases with increasing Graetz number is slowest for diffusion-limited antibody transport (Figure 3A). Figure 3A shows the predicted dimensionless clearance, relative to the predicted dimensionless clearance at Graetz number equal to 10, as a function of the Graetz number. The predicted dimensionless clearance is shown in normalized form to allow visual comparison of simulations at different Damköhler numbers. For a Damköhler number of 1, increasing the Graetz number from 10 to 50 causes a 74% reduction in the predicted dimensionless clearance; for diffusion-limited antibody transport, the same increase in the Graetz number causes only a 56% reduction in the predicted dimensionless clearance. For this reason, the increase in predicted clearance with increasing antibody solution flow rate is greatest for diffusion-limited antibody transport (Figure 3B). For a SAF with the same geometry as the prototypes used in our in vitro studies, increasing the flow rate from 50 to 100 mL/min increases the predicted clearance from 15.0 to 17.0 mL/min (12.5%) when the Damköhler number is equal to 1, and from 33.6 to 47.6 mL/min (34%) when the antibody transport is diffusion-limited. Therefore diffusion-limited antibody transport is doubly advantageous, producing the highest clearance at a given antibody solution flow rate and the greatest increase in clearance when the antibody solution flow rate is raised.

Experimental Antibody Removal. During each anti-BSA removal experiment, the anti-BSA concentration at the SAF outlet increased sharply with the first 200 mL of throughput (volume of antibody solution perfused through the SAF) as the priming solution was flushed from the perfusion system (Figure 4). The outlet concentration remained relatively constant for the remainder of the experiment (up to 800 mL throughput), indicating that the increase in bound anti-BSA concentration during the experiment was negligible compared to the anti-BSA-binding capacity of the SAF (i.e., c_b^* was near zero throughout the experiment).

As expected for c_b^* approximately equal to zero, the anti-BSA clearance was independent of anti-BSA inlet concentration for inlet concentrations between 0.5 and 2

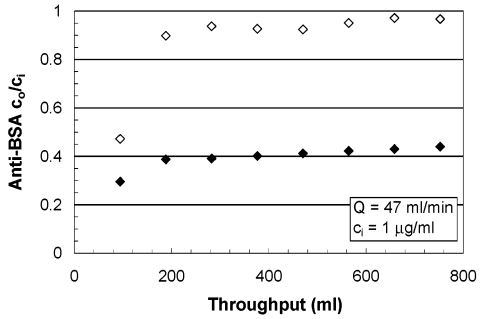

Figure 4. Anti-BSA outlet concentration relative to inlet concentration (c_o/c_i) during a typical anti-BSA removal experiment. Throughput is the volume of anti-BSA solution perfused through the SAF. Open symbols indicate data for a control SAF with immobilized HSA; closed symbols indicate data for a test SAF with immobilized BSA. Each experiment was performed at an anti-BSA solution flow rate of 47 mL/min and an anti-BSA inlet concentration of 1 μg/mL.

μg/mL (Figure 5). At an anti-BSA solution flow rate of 47 mL/min, the average of the clearances measured at inlet concentrations of 0.5, 1, and 2 μg/mL was 26.3 mL/min and the nonspecific clearance by the control SAF (at an inlet concentration of one μg/mL) was 2.8 mL/min. The measured clearance using the SAFs with immobilized BSA, minus the nonspecific clearance, was approximately 73% of the predicted diffusion-limited clearance and was within 2% of the clearance predicted for Damköhler number equal to 3.

Anti-BSA clearance increased to 36.2 mL/min when the anti-BSA solution flow rate was raised to 110 mL/min (Figure 6). The nonspecific clearance by the control SAF was 6.8 mL/min at an anti-BSA solution flow rate of 110 mL/min. The measured clearance using the SAF with immobilized BSA, minus the nonspecific clearance, was approximately 60% of the predicted diffusion-limited clearance and was within 5% of the clearance predicted for Damköhler number equal to 3.

At an anti-BSA solution flow rate of 47 mL/min, the anti-BSA clearance decreased to 16.2 mL/min when the anti-BSA-binding capacity decreased by approximately 50% (by immobilizing HSA and BSA within the SAF instead of BSA only) (Figure 7). The measured anti-BSA clearance using the SAF with immobilized HSA and BSA, minus the nonspecific clearance by the control SAF, was within 10% of the clearance predicted for Damköhler number equal to 1.

Discussion

Transport of anti-BSA antibodies in SAF prototypes with immobilized BSA occurred in the intermediate

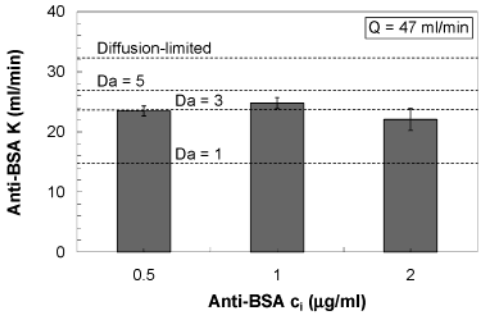

Figure 5. Dependence of anti-BSA clearance (*K*) on anti-BSA inlet concentration (c_i). Each experiment was performed at an anti-BSA solution flow rate of 47 mL/min. Dashed lines indicate the predicted clearances for Damköhler numbers (*Da*) of 1, 3, and 5, and for diffusion-limited antibody transport. For each simulation the dimensionless concentration of bound antibodies is equal to zero.

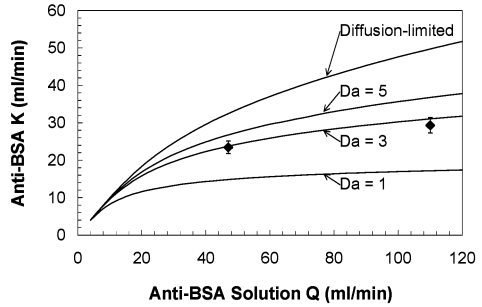

Figure 6. Dependence of anti-BSA clearance (*K*) on anti-BSA solution flow rate (*Q*). Simulated dependences of clearance on flow rate, for Damköhler numbers (*Da*) of 1, 3, and 5 and for diffusion-limited antibody transport, are also shown. For each simulation the dimensionless concentration of bound antibodies is equal to zero.

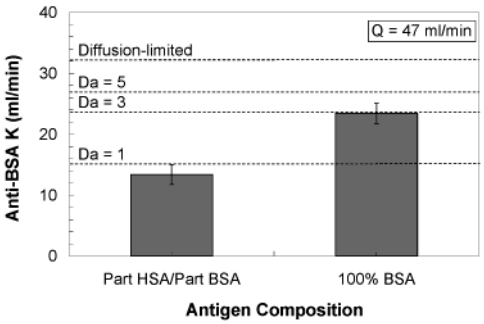

Figure 7. Dependence of anti-BSA clearance (*K*) on antigen composition. Each experiment was performed at an anti-BSA solution flow rate of 47 mL/min. Dashed lines indicate the predicted clearances for Damköhler numbers (*Da*) of 1, 3, and 5 and for diffusion-limited antibody transport. For each simulation the dimensionless concentration of bound antibodies is equal to zero.

regime, at a Damköhler number approximately equal to 3, and hence both the anti-BSA-binding rate and the radial anti-BSA diffusion rate were important determinants of the anti-BSA removal rate and clearance. At anti-BSA solution flow rates of 47 and 110 mL/min, we found close agreement between the measured anti-BSA clearances and the model-predicted clearances for Damköhler number equal to 3. Additionally, the anti-BSA clearance was highly dependent on the anti-BSA-binding capacity of the SAF, as expected for transport in the intermediate regime. Based on our initial estimates of the expected Damköhler number for SAF-based IgG removal, we expected the anti-BSA transport in the SAF prototypes to be diffusion-limited. Several factors may have contributed to the low Damköhler number achieved in our model system. In our SAF prototypes, BSA was immobilized on the fibers via accessible primary amines on the BSA. Since BSA contains 59 primary amine-containing lysine residues (*29*), of which about 30−35 are on the surface and available as immobilization points (*41*), the population of immobilized BSA was heterogeneous and a fraction of the immobilized BSA may have been unable to bind anti-BSA. Additionally, immobilization of the BSA may have reduced the intrinsic anti-BSA/BSA association rate constant and produced a low affinity antibody−antigen system. Finally, the anti-BSA population used may have had a low intrinsic affinity for BSA. Several antigens used for immunoadsorption are available in synthetic form and can be immobilized via spacer molecules to ensure that most of the epitopes are accessible to the antibodies (*42, 43*). SAFs containing these antigens may have antibody-binding capacities high enough to produce diffusion-limited transport of medium and high affinity antibodies ($k_f \geq 0.1$ mL/nmol·s or 10^5 L/mol·s). During the development of SAFs for clinical use, equilibrium antibody-binding experiments must be performed to measure the antibody-binding capacity of the SAF and to ensure that the immobilization method is optimized to produced the highest possible antibody-binding capacity.

Our antibody transport model can be used to predict the SAF-based antibody removal rate if the SAF geometry, blood flow rate, antibody diffusivity, and antibody-binding rate are known. The model can also be used to help assess how close a given system is to achieving diffusion-limited antibody transport. For example, if the anti-BSA/BSA system were a system of clinical relevance, we would continue the SAF prototype development with the goal of tripling the anti-BSA-binding capacity of the SAF fibers and increasing the Damköhler number to 9. Further development to increase the Damköhler number past 9 or 10 would be unwarranted, since the model predicts little enhancement in clearance obtained by raising the Damköhler number above 10.

Our transport model does not consider the inherent heterogeneity of polyclonal antibodies. As antibody populations do not display a Gaussian distribution of affinities in vivo (*44*), appropriate mathematical representation of antibody heterogeneity is difficult and requires extensive knowledge of the antibody/antigen system being studied. Use of an "average" value for k_f may overpredict the clearance since the clearance depends nonlinearly on k_f (i.e., the slow clearance of low affinity antibodies is not balanced by the fast clearance of high affinity antibodies).

Radial antibody convection due to ultrafiltration of buffer or plasma water across the fiber walls may increase the SAF-based antibody removal rate, especially if the antibody transport is diffusion-limited in the absence of radial convection. The radial Peclet number (Pe_r) represents the ratio of the characteristic radial antibody convective velocity to the characteristic radial antibody diffusive velocity (*22*): $Pe_r = v_{uf}a/D$, where v_{uf} (cm/s) is the radial convective velocity of the buffer or plasma water at the inner fiber walls. For the Hemophan fibers used in this study, a transmembrane pressure of up to 500 mmHg can be safely induced, producing a radial convective velocity at the inner fiber walls of up to 1×10^{-4} cm/s (*24*). At this radial convective velocity the radial Peclet number for IgG removal is equal to 2.5, and hence the radial antibody convective velocity is comparable to the radial antibody diffusive velocity and ultrafiltration may raise the antibody removal rate.

During each in vitro antibody removal experiment performed for this study, the shell compartment of the SAF was filled with isotonic buffer and closed and hence the net ultrafiltration rate was zero. The magnitude of the Starling recirculation (recirculation between the blood and shell compartments due to the drop in hydrostatic pressure along the length of each fiber) was small compared to the antibody solution flow rate since the ratio of the lumenal flow resistance to the transmembrane flow resistance was much less than 1 (*45*). The maximum radial Peclet number (at the SAF inlet and outlet) due to Starling recirculation was 0.04, and hence Starling recirculation did not affect the measured anti-BSA removal rates.

The SAF-based antibody removal rate from whole blood will differ from the removal rate from buffer, since the antibody-binding rate and the antibody radial diffusion rate will have different magnitudes in blood and in buffer. Nonspecific binding of plasma proteins present at high concentrations in whole blood may reduce the antibody-binding rate in blood compared to the binding rate in buffer. In stagnant blood, the antibody diffusivity will be less than the diffusivity in buffer; however, due to shear-enhanced diffusion the antibody diffusivity in flowing whole blood may be higher than the diffusivity in buffer (*46*). Additional mathematical and experimental studies are required to determine the relationship between the antibody removal rate from buffer and the antibody removal rate from whole blood.

Acknowledgment

This work was supported in part by the NIH National Institute of Diabetes and Digestive and Kidney Diseases under grant R44 DK54122, awarded to Advanced Extravascular Systems. We greatly appreciate the generous support of Advanced Extravascular Systems, the McGowan Institute for Regenerative Medicine, and the Provost of the University of Pittsburgh.

References and Notes

(1) Tanabe, K.; Takahashi, K.; Sonda, K.; Tokumoto, T.; Ishikawa, N.; Kawai, T.; Fuchinoue, S.; Oshima, T.; Yagisawa, T.; Nakazawa, H.; Goya, N.; Koga, S.; Kawaguchi, H.; Ito, K.; Toma, H.; Agishi, T.; Ota, K. Long-Term Results of ABO-Incompatible Living Kidney Transplantation−A Single-Center Experience. *Transplantation* **1998**, *65*, 224−228.

(2) Cooper, D. K.; Human, P. A.; Lexer, G.; Rose, A. G.; Rees, J.; Keraan, M.; Du Toit, E. Effects of Cyclosporine and Antibody Adsorption on Pig Cardiac Xenograft Survival in the Baboon. *J. Heart Transplant.* **1988**, *7*, 238−246.

(3) Xu, Y.; Lorf, T.; Sablinski, T.; Gianello, P.; Bailin, M.; Monroy, R.; Kozlowski, T.; Awwad, M.; Cooper, D. K. C.; Sachs, D. H. Removal of Anti-Porcine Natural Antibodies from Human and Nonhuman Primate Plasma in Vitro and in Vivo by a Gal Alpha 1-3gal Beta 1-4 Beta Glc-X Immunoaffinity Column. *Transplantation* **1998**, *65*, 172−179.

(4) Kluth, D. C.; Rees, A. J. Anti-Glomerular Basement Membrane Disease. *J. Am. Soc. Nephrol.* **1999**, *10*, 2446−2453.

(5) Benny, W. B.; Sutton, D. M.; Oger, J.; Bril, V.; McAteer, M. J.; Rock, G. Clinical Evaluation of a Staphylococcal Protein A Immunoadsorption System in the Treatment of Myasthenia Gravis Patients. *Transfusion* **1999**, *39*, 682−687.

(6) Knobl, P.; Derfler, K. Extracorporeal Immunoadsorption for the Treatment of Haemophilic Patients with Inhibitors to Factor VIII or IX. *Vox Sang* **1999**, *77 Suppl 1*, 57−64.

(7) Snyder, H. W., Jr.; Cochran, S. K.; Balint, J. P., Jr.; Bertram, J. H.; Mittelman, A.; Guthrie, T. H., Jr.; Jones, F. R. Experience with Protein A-Immunoadsorption in Treatment-Resistant Adult Immune Thrombocytopenic Purpura. *Blood* **1992**, *79*, 2237−2245.

(8) Madore, F. Plasmapheresis. Technical Aspects and Indications. *Crit. Care Clin.* **2002**, *18*, 375−392.

(9) Matic, G.; Bosch, T.; Ramlow, W. Background and Indications for Protein A-Based Extracorporeal Immunoadsorption. *Ther. Apheresis* **2001**, *5*, 394−403.

(10) Nydegger, U. E.; Rieben, R.; Mohacsi, P. Current Precision of Immunological Extracorporeal Plasma Treatment. *Transfus Apheresis Sci.* **2001**, *24*, 39−47.

(11) Braun, N.; Bosch, T. Immunoadsorption, Current Status and Future Developments. *Expert Opin. Invest. Drugs* **2000**, *9*, 2017−2038.

(12) Bertram, J. H.; Jones, F. R.; Balint, J. P., Jr. Protein A Immunoadsorption. *Clin. Immunother.* **1996**, *6*, 211−227.

(13) Hout, M. S.; LeJeune, K. E.; Schaack, T. M.; Bristow, D. K.; Federspiel, W. J. Specific Removal of Anti-A and Anti-B Antibodies by Using Modified Dialysis Filters. *ASAIO J.* **2000**, *46*, 702−706.

(14) Hout, M. S. Selective Antibody Removal from Blood, Plasma, and Buffer Using Hollow Fiber-Based Specific Antibody Filters. Ph.D. Dissertation, University of Pittsburgh, 2003.

(15) Singh, P.; Goldman, J.; Jackson, C. E. Preparation and In Vitro Evaluation of a New Extracorporeal Dialyzer with Immobilized Insulin. *Artif. Organs* **1982**, *6*, 145−150.

(16) Larue, C.; Gueraud, V.; Rivat, C. Suitable Hollow Fibre Immunobioreactors for Specific Ex Vivo Removal of Antibodies and Antigens from Plasma. *Clin. Exp. Immunol.* **1985**, *62*, 217−224.

(17) Yang, V. C.; Port, F. K.; Kim, J. S.; Teng, C. L.; Till, G. O.; Wakefield, T. W. The Use of Immobilized Protamine in Removing Heparin and Preventing Protamine-Induced Complications During Extracorporeal Blood Circulation. *Anesthesiology* **1991**, *75*, 288−297.

(18) Ma, X.; Mohammad, S. F.; Kim, S. W. Heparin Removal from Blood Using Poly(L-Lysine) Immobilized Hollow Fiber. *Biotechnol. Bioeng.* **1992**, *40*, 530−536.

(19) Karoor, S.; Molina, J.; Buchmann, C. R.; Colton, C.; Logan, J. S.; Henderson, L. W. Immunoaffinity Removal of Xenoreactive Antibodies Using Modified Dialysis or Microfiltration Membranes. *Biotechnol. Bioeng.* **2003**, *81*, 134−148.

(20) Klein, E.; Eichholz, E.; Yeager, D. H. Affinity Membranes Prepared from Hydrophilic Coatings on Microporous Polysulfone Hollow Fibers. *J. Membr. Sci.* **1994**, *90*, 69−80.

(21) Charcosset, C.; Su, Z.; Karoor, S.; Daun, G.; Colton, C. K. Protein A Immunoaffinity Hollow Fiber Membranes for Immunoglobulin G Purification: Experimental Characterization. *Biotechnol. Bioeng.* **1995**, *48*, 415−427.

(22) Cussler, E. L. *Diffusion: Mass Transfer in Fluid Systems*, 2nd ed.; Cambridge University Press: Cambridge, New York, 1997.

(23) Bamford, C. H.; Al-Lamee, K. G.; Purbrick, M. D.; Wear, T. J. Studies of a Novel Membrane for Affinity Separations. *J. Chromatogr.* **1992**, *606*, 19−31.

(24) *Instructions for Use of Hemodialyzers*; Gambro: Lakewood, CO.

(25) Yarmush, D. M.; Murphy, R. M.; Colton, C. K.; Fisch, M.; Yarmush, M. L. Quasi-Elastic Light Scattering of Antigen−Antibody Complexes. *Mol. Immunol.* **1988**, *25*, 17−32.

(26) Kuby, J. *Immunology*, 3rd ed.; W. H. Freeman: New York, 1997.

(27) Yarmush, M. L.; Patankar, D. B.; Yarmush, D. M. An Analysis of Transport Resistances in the Operation of Biacore; Implications for Kinetic Studies of Biospecific Interactions. *Mol. Immunol.* **1996**, *33*, 1203−1214.

(28) Chase, H. A. Affinity Separations Utilising Immobilised Monoclonal Antibodies−A New Tool for the Biochemical Engineer. *Chem. Eng. Sci.* **1984**, *39*, 1099−1125.

(29) Peters, T., Jr. Serum Albumin. *Adv. Protein. Chem.* **1985**, *37*, 161−245.

(30) Welty, J. R.; Wicks, C. E.; Wilson, R. E. *Fundamentals of Momentum, Heat, and Mass Transfer*, 3rd ed.; Wiley: New York, 1984.

(31) Deen, W. M. *Analysis of Transport Phenomena*; Oxford University Press: New York, 1998.

(32) Fournier, R. L. *Basic Transport Phenomena in Biomedical Engineering*; Taylor & Francis: Philadelphia, 1999.

(33) Sargent, J. A.; Gotch, F. A. Principles and Biophysics of Dialysis. In *Replacement of Renal Function by Dialysis*, 4th ed.; Jacobs, C., Kjellstrand, C. M., Koch, K. M., Winchester, J. F., Eds.; Kluwer Academic Publishers: Dordrecht, 1996.
(34) Skelland, A. H. P. *Diffusional Mass Transfer*; Wiley: New York, 1974.
(35) von Sengbusch, G.; Lemke, H. D.; Vienken, J. Evolution of Membrane Technology: Possibilities and Consequences. In *Uremia Therapy*; Gurland, H. J., Ed.; Springer-Verlag: Berlin, 1987.
(36) Colton, C. K.; Lysaght, M. J. Membranes for Hemodialysis. In *Replacement of Renal Function by Dialysis*, 4th ed.; Jacobs, C., Kjellstrand, C. M., Koch, K. M., Winchester, J. F., Eds.; Kluwer Academic Publishers: Dordrecht, 1996.
(37) Axen, R.; Porath, J.; Ernback, S. Chemical Coupling of Peptides and Proteins to Polysaccharides by Means of Cyanogen Halides. *Nature* **1967**, *214*, 1302−1304.
(38) Crowther, J. R. *The ELISA Guidebook*; Humana Press: Totowa, NJ, 2001.
(39) al-Yaman, F.; Genton, B.; Falk, M.; Anders, R. F.; Lewis, D.; Hii, J.; Beck, H. P.; Alpers, M. P. Humoral Response to Plasmodium Falciparum Ring-Infected Erythrocyte Surface Antigen in a Highly Endemic Area of Papua New Guinea. *Am. J. Trop. Med. Hyg.* **1995**, *52*, 66−71.
(40) Kozlowski, T.; Ierino, F. L.; Lambrigts, D.; Foley, A.; Andrews, D.; Awwad, M.; Monroy, R.; Cosimi, A. B.; Cooper, D. K.; Sachs, D. H. Depletion of Anti-Gal(Alpha)1-3gal Antibody in Baboons by Specific Alpha-Gal Immunoaffinity Columns. *Xenotransplantation* **1998**, *5*, 122−131.
(41) *Instructions for Imject Carrier Proteins BSA, KLH, and OVA*; Pierce Chemical Company: Rockford, IL.
(42) Rieben, R.; Korchagina, E. Y.; von Allmen, E.; Hovinga, J. K.; Lammle, B.; Jungi, T. W.; Bovin, N. V.; Nydegger, U. E. In Vitro Evaluation of the Efficacy and Biocompatibility of New, Synthetic ABO Immunoabsorbents. *Transplantation* **1995**, *60*, 425−430.
(43) Gerber, B.; Tinguely, C.; Bovin, N. V.; Rieben, R.; Nydegger, U. E. Differences between Synthetic Oligosaccharide Immunoabsorbents in Depletion Capacity for Xenoreactive Anti-Galalpha1-3gal Antibodies from Human Serum. *Xenotransplantation* **2001**, *8*, 106−114.
(44) Roitt, I. M.; Brostoff, J.; Male, D. K. *Immunology*, 4th ed.; Mosby: London, Baltimore, 1996.
(45) Bruining, W. J. A General Description of Flows and Pressures in Hollow Fiber Membrane Modules. *Chem. Eng. Sci.* **1989**, *44*, 1441−1447.
(46) Wang, N. H. L.; Keller, K. H. Augmented Transport of Extracellular Solutes in Concentrated Erythrocyte Suspensions in Couette Flow. *J, Colloid Interface Sci.* **1985**, *103*, 210−225.

Accepted for publication May 30, 2003.

BP025796F